



HAL
open science

Paleomagnetic full vector record of four consecutive Mid Miocene geomagnetic reversals

J. Linder, R. Leonhardt

► **To cite this version:**

J. Linder, R. Leonhardt. Paleomagnetic full vector record of four consecutive Mid Miocene geomagnetic reversals. *Physics of the Earth and Planetary Interiors*, 2009, 177 (1-2), pp.88. 10.1016/j.pepi.2009.07.013 . hal-00585470

HAL Id: hal-00585470

<https://hal.science/hal-00585470>

Submitted on 13 Apr 2011

HAL is a multi-disciplinary open access archive for the deposit and dissemination of scientific research documents, whether they are published or not. The documents may come from teaching and research institutions in France or abroad, or from public or private research centers.

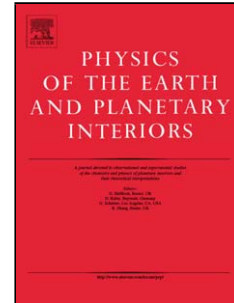
L'archive ouverte pluridisciplinaire **HAL**, est destinée au dépôt et à la diffusion de documents scientifiques de niveau recherche, publiés ou non, émanant des établissements d'enseignement et de recherche français ou étrangers, des laboratoires publics ou privés.

Accepted Manuscript

Title: Paleomagnetic full vector record of four consecutive
Mid Miocene geomagnetic reversals

Authors: J. Linder, R. Leonhardt

PII: S0031-9201(09)00156-3
DOI: doi:10.1016/j.pepi.2009.07.013
Reference: PEPI 5188



To appear in: *Physics of the Earth and Planetary Interiors*

Received date: 31-7-2008
Revised date: 14-7-2009
Accepted date: 16-7-2009

Please cite this article as: Linder, J., Leonhardt, R., Paleomagnetic full vector record of four consecutive Mid Miocene geomagnetic reversals, *Physics of the Earth and Planetary Interiors* (2008), doi:10.1016/j.pepi.2009.07.013

This is a PDF file of an unedited manuscript that has been accepted for publication. As a service to our customers we are providing this early version of the manuscript. The manuscript will undergo copyediting, typesetting, and review of the resulting proof before it is published in its final form. Please note that during the production process errors may be discovered which could affect the content, and all legal disclaimers that apply to the journal pertain.

Paleomagnetic full vector record of four consecutive Mid Miocene geomagnetic reversals

J. Linder ^{*}, R. Leonhardt [◇]

^{*} *Department for Earth and Environmental Sciences,
Ludwig-Maximilians-University, Munich, Germany*

[◇] *Institute for Geophysics, Montanuniversität Leoben, Austria*

Abstract

Seventy Mid Miocene lava flows from flood basalt piles near Neskaupstadur (East Iceland) were sampled, which provide a quasi-continuous record of geomagnetic field variations. Samples were collected along the Profile B of Watkins and Walker (1977), which was extended about 250 m farther down in a neighboring stream bed. Published radiometric age determinations (Harrison et al., 1979) range from 12.2 to 12.8 Ma for the sampled sequence. Four reversals were recorded in this profile, with 18 transitional lavas found within or between 17 normal and 30 reversed polarity flows. The large amount of transitional lavas and the large virtual geomagnetic pole dispersion for stable field directions are noteworthy as such features are commonly observed in Icelandic lavas and manifest in a far-sidedness of the average VGP. The reason for this characteristic, which could be related to an anomaly beneath Iceland, a global field phenomenon, local tectonics, and/or non-horizontal flow emplacement, is scrutinized. Non-horizontal flow emplacement is likely in volcanic environments particularly if the sampled lavas are located on the paleoslopes of a central volcano.

From the difference of the observed paleomagnetic mean directions to the expected directions assuming a geocentric axial dipole (GAD), a paleoslope which would explain the observed difference was calculated numerically. The obtained dip and dip direction point consistently to a possible volcanic extrusion center of the lavas. The determined paleodip, however, proved to be significantly too high compared to the usual slope of a central volcano, suggesting further reasons for deviations from the GAD. Other datasets of this age from Europe also show enhanced VGP dispersion, suggesting further contributions of geomagnetic origin for this observation. Basically all reversal paths move across the Pacific. Transitions were identified as belonging to C5An.1r - C5Ar.3r based on the Astronomically Tuned Neogene Timescale (Lourens et al., 2004). We selected 122 samples for paleointensity measurements using a modified Thellier method including tests for alteration and multidomain bias. 85 of the measured samples yielded data of sufficient quality to calculate paleointensities for 26 lava flows. The average paleointensity for stable field directions was $23.3 \mu\text{T}$, whereas the intensity drops to a minimum of $5.8 \mu\text{T}$ during field transitions. The stable field intensities represent only about half of the present day field. The saw-tooth pattern of intensities, which is characterized by a sharp increase of intensity directly after a reversal and then followed by a gradual decrease towards the next reversal, was not found in this study.

Key words:

Paleomagnetism, absolute paleointensity, Eastern Iceland, Mid Miocene, Geomagnetic reversals

Email address: julia.linder@geophysik.uni-muenchen.de (J. Linder *).

1 **1 Introduction**

2 The Earth's magnetic field has changed its polarity many times in the past.
3 It is not known in detail how the geomagnetic field behaves during a reversal,
4 but many results show a decrease of field intensity, likely related to a de-
5 creased dipole component, and multipole components, which become stronger
6 (e.g. Merrill and McFadden, 1999; Leonhardt and Fabian, 2007). Detailed
7 records of transitional fields were mostly obtained from sediments. In the
8 work of Clement (1991), Tric et al. (1991) and Laj et al. (1991) the tran-
9 sitional VGPs were predominantly found within two approximately antipodal
10 longitudinal bands across America and Asia. Some theories state the existence
11 of this preferred longitudes of the virtual geomagnetic poles (VGPs) due to
12 local flux concentrations of radial components and lower temperatures at the
13 CMB. However, other studies (Prévot and Camps, 1993; Langereis et al., 1992;
14 Leonhardt and Fabian, 2007) could not confirm these preferred longitude sec-
15 tors. Beside geomagnetic reversals, the field behavior during stable polarities
16 is subject of detailed research. The field's intensity was found to follow an
17 asymmetric saw tooth pattern, which is characterized by a decrease before
18 reversals and a large sudden recovery after the polarity change (Valet and
19 Meynadier, 1993). However, remanences in sediments are often affected by
20 post-depositional reorientation and the magnetic torque acting on the parti-
21 cles may not be sufficient to orient them properly (Tauxe, 1993). Furthermore
22 the remanence acquisition can also be severely delayed (Roberts and Winkl-
23 hofer, 2004), if sedimentation rate is low. In contrast to sediments, volcanic
24 rocks record a geologically instantaneous field (Prévot et al., 1985) and provide
25 the possibility to determine absolute paleointensities. Unfortunately, volcanic

26 activity is usually very short lived and sporadic. Therefore, magnetic measure-
27 ments at volcanic sequences are often of weak temporal resolution and cover
28 only short time intervals.

29 Exceptional long time intervals, however, have been found particularly in Ice-
30 land (Watkins and Walker, 1977) and Kerguelen Archipelago (Camps et al.,
31 2007). The flood basalt piles in East Iceland, cover an enormous age range and
32 they are highly suitable for paleomagnetic measurements due to the extrusion
33 of one lava flow per 10 kyr, a mean extrusion rate which is assumed to be quite
34 homogenous in the lower part of the pile (Watkins and Walker, 1977). Previ-
35 ous paleomagnetic projects in Eastern Iceland are the work of Watkins and
36 Walker (1977) in Neskaupstadur and of Kristjansson (1995) at the neighbor-
37 ing peninsula. Watkins and Walker (1977) magnetostratigraphically correlated
38 700 successive lavas in the flood basalt pile, ranging from 13.6 to 2.0 Ma in
39 age. Herrero-Bervera et al. (1999) repeated the Watkins and Walker profiles
40 C and D (12.09-10.21 Ma) for a more detailed examination of transitional
41 lava flows and reversal paths. In this study, profile B of Watkins and Walker
42 (1977) was repeated and extended 200 m farther down to determine the direc-
43 tional behavior and absolute paleointensity variation across geomagnetic field
44 reversals, as well as to analyze the full vector record during stable polarity
45 intervals.

46 **2 Geological setting and field work**

47 Samples were taken from lava flows of the flood basalt pile mountain Nipokol-
48 lur (65.157 °N, 13.656 °W) near Neskaupstadur, Eastern Iceland. These flood
49 basalts are well stratified and dip towards the active zone due to spreading

50 (Walker, 1974). The regional dip in the flood basalts piles of Neskaupstadur
51 varies from 8° at sea level to 4° at mountain summits. On average this re-
52 gional dip decreases with $1\text{-}1.5^\circ$ per 200 m altitude (Kristjansson, 1995) due to
53 down-dip thickening of the lava flows (Walker, 1964). The average accumula-
54 tion rate of the basalt piles of 700-1000 m per Myr is decreasing with altitude.
55 Due to intensive erosion only 1200 m altitude of the originally 10 km thick
56 plateaus is left today (Krafft, 1984). Glaciers created the fjords in the Qua-
57 ternary (Kristjansson, 1995), leaving outstanding outcrops of the basalt piles.
58 In principle, we followed profile B of Watkins and Walker (1977) (see Fig. 1),
59 but extended it farther down to 199 m altitude (original profile was down to
60 550 m). With a total of 70 lava flows an altitude of about 500 m was covered.
61 Within the sampled profile some dykes (about 2 m wide) came close to the
62 sites. A minimum distance of 9 m was always kept to prevent a thermally
63 induced magnetic overprint of the dyke. Below site 20 we had to proceed the
64 profile in a neighboring stream bed, as a very broad dyke crosses the outcrops
65 of our section and the minimum distance could not be maintained anymore.
66 Within the section also pillow lavas were found, which presumably formed in
67 some shallow temporary ponds (Walker, 1974). Individual lavas were distin-
68 guished by red beds or paleosoils as well as top and basal breccia of the flow.
69 Six samples per site with a diameter of one inch (2.54 cm) were cored using
70 a gasoline-powered portable drill with a water-cooled diamond bit. Whenever
71 possible samples were drilled horizontally distant and in the lower third of a
72 lava flow in order to avoid any reheating from later flows above.

73 **3 Methods and Results**74 *3.1 Rock Magnetism*

75 For a preselection and eligibility testing of the samples for paleointensity de-
76 terminations, rock magnetic measurements were carried out for one sample
77 per site, including isothermal remanent magnetization (IRM) acquisition, back
78 field curves and hysteresis measurements with a peak field of 900 mT and ther-
79 momagnetic measurements with a peak temperature of 700 °C at the variable
80 field translation balance (VFTB) of Petersen instruments. Hysteresis mea-
81 surements revealed that most of the samples are within the PSD range and
82 cluster along the SD-MD mixture lines (Dunlop, 2002) (see Fig. 2). Thermo-
83 magnetic results are discussed in the following together with ore microscopy.
84 Furthermore, we performed measurements of the anisotropy of magnetic sus-
85 ceptibility on a representative part of the collection to test for the possibility
86 of anisotropy bias in paleointensity determination and to analyze the flow di-
87 rections of the lava flows (Henry et al., 2003). All investigated samples are
88 found to be isotropic, based on anisotropy values well below 1.5%.

89 *3.2 Thermomagnetic curves and ore microscopy*

90 Samples were classified into four groups based on microscopy and thermomag-
91 netic experiments (see Fig. 3). Ore microscopic observations of 14 samples
92 helped to determine the oxidation state of the magnetic rock and to identify
93 the remanence carriers.

94 Group 1 samples (5 % of samples) show two Curie temperatures, one around

95 200°C and the other at 450°C. The lower Curie temperature is likely related
96 to unoxidized regions in the titanomagnetites as shown in the ore microscopy
97 picture. Accumulation of ferrofluid along cracks in these titanomagnetites sug-
98 gests a secondary maghemitization, which is responsible for the second Curie
99 temperature.

100 The dominant Curie temperature of group 2 (10 %) range between 250°C and
101 430°C. As shown in the microscopy picture, cracks are abundant in the mag-
102 netic minerals, likely induced by shrinking during low temperature oxidation.

103 Therefore this magnetic phase is interpreted to be titanomaghemite. Skeletal
104 and cruciform structures can also be observed, which are a result of late crys-
105 tallization of the TM into an already firm matrix, typical for tholeiitic magmas
106 (Carmichel et al., 1960). Additionally, a minor amount of high temperature
107 oxidized grains are present, carrying a primary magnetization above 450°C.

108 Judging from ore microscopy, group 3 samples (25 %) are very similar to group
109 2 samples, except for the fact that the presence of a high temperature oxidized
110 titanomagnetite is clearly visible in the thermomagnetic curve.

111 Samples of group 4 (60 %)(Fig. 3) are characterized by single Curie temper-
112 atures between 500° and 580°C. Beautiful exsolution lamellae were found in
113 these samples, indicating high temperature oxidation. Highly oxidized phases
114 are relatively insensitive to further oxidation under laboratory conditions,
115 which is an excellent qualification for any paleomagnetic analysis. Only sam-
116 ples from sites, where this behavior was observed, were subjected to paleoin-
117 tensity determinations.

119 NRM measurements were carried out in the magnetically shielded laboratory
120 of the LMU in Niederlippach. A cryogenic magnetometer for the weaker mag-
121 netized samples and a spinner magnetometer for the stronger ones were used
122 to determine the samples' remanences. Half of the samples per site were sub-
123 jected to alternating field demagnetization (up to 200 mT) and the other half
124 was thermally demagnetized (up to 600 °C) with at least 14 steps. Measure-
125 ments of the susceptibility with a Geofyzika KLT-3 minikappa bridge after
126 every heating step helped to recognize the onset of chemical alteration of the
127 thermally treated samples. Typical demagnetization diagrams for normal, re-
128 versed and transitional directions are shown in Fig. 4a. For over 90 % of all
129 samples of Neskaupstadur the orthogonal projection is characterized by a sta-
130 ble directional component. Despite their age most samples only carry a minor
131 viscous overprint, which is demagnetized between 100 and 150 °C (see Fig. 4).
132 For some samples principle component analysis could not be applied. Those
133 directions were evaluated using great circle techniques (McFadden and McEl-
134 henny, 1988) (see Fig. 4b). Few samples contain a major magnetic overprint
135 or a unstable direction with a too small unaffected NRM to be evaluable (see
136 Fig. 4c). Only samples with a confidence cone $\alpha_{95} < 12^\circ$ and a concentration
137 parameter $k > 40$ (calculated using Fisher (1953) statistics) were included
138 into further evaluation of the paleodirections.

139 Tilt corrections had to be applied to the dataset, as the center of Iceland sub-
140 sided due to spreading effects and the weight of the glaciers and extrusions.
141 Thus, the flood basalt pile near Neskaupstadur has an regional tilt of about
142 4-8° to 264°W. In most previous studies (Watkins and Walker, 1977; Krist-

143 jansson, 1995; Herrero-Bervera et al., 1999) it is assumed that the flood basalts
144 flow over very far distances with negligible slope and were emplaced subhor-
145 izontally. Therefore a tilt correction to horizontal is applied to the Tertiary
146 basalt piles in Eastern and Western Iceland with a dip direction pointing
147 towards the central ridge and a dip varying with altitude due to down-dip
148 thickening. The same approach is used here for initial analysis and its valid-
149 ity will be discussed below. By linear interpolation the dip values of the lava
150 flows were calculated to vary from 7 ° for the sites JD-10 (150-300 m), 6 ° for
151 the sites 11-25 (300-450 m), 5 ° for the sites 27-45 (450-600 m) to 4 ° for the
152 uppermost sites 46-64 (600-761 m).

153 Four reversals were found within the section (see Fig. 5) with the transitional
154 directions of the sites 51-46B (denoted reversal D below), 36-29 (reversal C),
155 16-14 (reversal B) and 11-05(reversal A). The sites 62-58 are assumed to repre-
156 sent an excursion, the sites 00-JD could indicate the termination of a preceding
157 reversal. Using a cut-off colatitude for transitional lavas of 41.3 ° (McElhinny
158 and McFadden, 1997) we found 18 transitional, 30 reversed and 17 normal
159 polarities in the section. From 6 sites no reliable paleodirection could be de-
160 rived. At a first glance the inclinations represent the expected values of a GAD
161 pretty well (see Fig. 5). The declination scatters, but this is a typical feature
162 at high latitudes.

163 Numerous dykes are found within the lava pile of eastern Iceland. In our profile,
164 the minimum distance between dyke and sampling locality was 9 m (for the
165 sampling spot at flow JD). In order to identify any possible magnetic overprint
166 by later intrusion of this 5 m thick dyke, this dyke was sampled as well (site
167 DY). Different directions between dyke and lava flow indicate that his dyke did
168 not affect the remanence at our our sampling spot. The possible influence of

169 dyke reheating was also investigated by a contact test close to site 13. This lava
170 flow is crossed by a relatively thin dyke ($\approx 3\text{m}$). Four samples were taken from
171 the dyke itself, another four in increasing distances (0.7 to 2.6 m) from the
172 dyke. All samples show a similar directed and relatively strong overprint up to
173 370°C . Above this temperature distinctively different directions are observed
174 between dyke and lava flow, already at closest distance of 0.7 m. Most dykes
175 along the sampled profile are of similar or less width compared to the dyke
176 crossing the section at site 13. Thus the minimum distance of more than 9 m
177 to the dyke, which was kept for all sites, is sufficient to prevent sampling of
178 reheated rocks.

179 *3.4 Paleointensities*

180 The intensity of the TRM in the flood basalts depends on the amount of mag-
181 netic minerals, their composition, grain size and grain shape, the decay of the
182 magnetization with time and, of course, the ancient magnetic field. For the
183 paleointensity measurements in this study the MT4 method (modified Thellier
184 type four, containing alteration (CK), tail (TR) and additivity checks (AC))
185 (Leonhardt et al., 2004) was used. The laboratory field inside the shielded fur-
186 nace, applied during heating and cooling, was chosen to be $30\ \mu\text{T}$, about half of
187 the present day field, because of the high amount of transitional lavas and due
188 to the presumed Miocene dipole low (Prévot et al., 1985). The samples of 8mm
189 diameter and 7mm length were magnetized along the z-axis and kept in the
190 same position within in the furnace during all temperature steps to minimize
191 bias from temperature gradients and field variations. Due to the small sample
192 size slightly larger orientation errors occur in the x-y plane, leading to more

193 scattered horizontal components on the orthogonal projections. Paleointensity
194 determinations, however, are unaffected. ThellierTool4.11 (Leonhardt et al.,
195 2004) was used to analyze the paleointensity determinations. All analyzes are
196 characterized by origin pointing stable directional component in agreement
197 with its directional analysis, NRM fractions f above 30% (average 73%), at
198 least 5 successive data point, quality factors q above 2.3 (average 15.8), minor
199 alteration contribution ($< 10\%$) determined both from the individual check
200 differences and from the cumulative difference, and finally, the absence of any
201 significant MD contribution as tested by tail checks ($\delta t^* < 5\%$ below the maxi-
202 mum unblocking temperature) and additivity checks. For a determination of a
203 site mean value, only sites with more than two eligible samples were accepted.
204 If more than two successful determinations are available for a site, then a
205 weighted mean of the paleointensity and its uncertainty was calculated using
206 the quality factor q (Coe et al., 1978) in order to emphasize intensity determi-
207 nations of higher quality. For six sites only 2 determinations were successful,
208 thus, the maximum possible uncertainty is given there. Tab. 2 summarizes
209 the paleointensity results for the all measured samples. Magnetomineralogical
210 changes during heating are the main reason for rejecting individual measure-
211 ments. For some weakly affected samples corrections for these alterations were
212 applied (Valet et al., 1996) using the cumulative alteration difference if any
213 significant contribution from MD remanence could be excluded based on tail
214 checks. Furthermore, check corrected samples (for an explanation of the cumu-
215 lative alteration difference see Leonhardt et al. (2004)) were only included if
216 additivity checks then fit the expected pTRM values suggesting a preservation
217 of essential TRM properties despite laboratory magnetomineralogical changes
218 and if at least one value per site could be determined without corrections. One
219 third of the collection was analyzed by applying the correction technique. The

220 mean paleointensity of $23.3 \mu\text{T}$ for stable polarities across the section is very
221 low. The values including reversals range from a minimum of $5.8 \mu\text{T}$ at site
222 32 to $22.8 \mu\text{T}$ at site jb and their average with $13.3 \mu\text{T}$ is about half of the
223 non-transitional periods.

224 4 Discussion

225 4.1 *Stable polarity fields*

226 **Magnetostratigraphic correlation.** Due to their stratigraphic succession,
227 the flood basalt piles in Eastern and Western Iceland provide an independent
228 geomagnetic timescale back to 13 Myr ago (Harrison et al., 1979), which can be
229 correlated with marine magnetic anomalies. At first we compared our data to
230 the results of profiles A and B of Watkins and Walker (1977), which are based
231 on two measurements for each directional unit. Based on flow descriptions,
232 similar altitude, and their position relative to pronounced red beds, some lava
233 flows (see Table 1) could be unambiguously correlated to profile B of Watkins
234 and Walker (1977). Above these flows a direct flow-to-flow correlation between
235 Watkins and our work is not possible, because of slightly different sampling
236 routes. Based on altitude measurements, however, both profiles can be com-
237 pared and paleodirectional comparisons yield mostly similar results, although
238 some differences in particular for transitional directions are also observed.
239 Watkins sampled older lava flows down to sea level in a different stream bed
240 some hundred meters to the east, denoted profile A (Watkins and Walker,
241 1977). Based on directional results, our data shows similar prominent features
242 as a composite A+B section of Watkins and Walker (1977). One discordance

243 concerns the 12d chron (Opdyke, 1972). Instead of a normal polarized site
244 at this altitude as stated by Watkins and Walker (1977) we found a tran-
245 sitional VGP in the northern hemisphere. The normal directions could have
246 been missed due to gaps (35m gap between site 10 and 11 and 60m between
247 site 13 and 14) in our section. Another possibility would be the insufficient
248 demagnetization in the previous work and thus, no 12d normal chron in the
249 previously sampled section. Correlation to global timescales like the Astro-
250 nomically Tuned Neogene Timescale ATNTS2004 (Lourens et al., 2004)(see
251 Fig. 7) and radiometric dating of overlying and underlying profiles (McDougall
252 and Schmincke, 1976; Harrison et al., 1979) give an age ranging from 12.2 to
253 12.8 Ma for the section, which is within the marine anomaly 5A. Based on
254 this correlation the sampled section ranges from C5Ar.2r to C5An.1r.

255 **Deviations from GAD field.** A positive class B reversal test confirmed that
256 the mean values of the normal and reversed polarity data show a good antipo-
257 dality, indicating that no overprints, insufficiently removed secondary compo-
258 nents or rotations falsify the VGPs. Although statistically not significant as
259 the uncertainty ellipse includes the geographic pole, the average normal and
260 reversed VGPs yield a slight right-handedness. Such right-handedness, how-
261 ever, can be observed in data from all over Iceland, independent of age and
262 location (Kristjansson and Jonsson, 2007). As the right-handedness is inde-
263 pendent of the location in Iceland and found in Eastern and Western Iceland,
264 neither rotational effects nor relocalization due to spreading can be the cause.
265 Some suggested possible explanations are a magnetic anomaly beneath Iceland
266 (Kristjansson and Jonsson, 2007), maybe connected to the plume, or a per-
267 sistent non axial-dipole field. All VGPs within the cut-off colatitude of 41.3°
268 (McElhinny and McFadden, 1997) were used to determine the VGP scatter

269 around the spin axis. McElhinny and McFadden (1997) proposed a angular
270 standart deviation of 20.2° for latitudes between 60° and 70° for the last 5 Myr.
271 In this study we determined a a slightly enhanced between site angular stan-
272 dard deviation of 23.2° with upper and lower confidence limits of 30.2° and
273 18.9° (Cox, 1969).

274 The VGP latitudes in this study show a tendency to decrease from the moun-
275 tain tops to the sea level . However, as will be shown in the following, these
276 low VGP latitudes are an artefact due to the applied dip correction based on
277 the assumption of horizontal emplacement of the lavas. If there was an initial
278 topography like central volcanoes, which can have a slope up to 10° , then
279 the flood basalts already had an initial dip during deposition and correction
280 towards horizontal emplacement falsifies the result. Also the down-dip thick-
281 ening (Walker, 1964) of the lava flows suggests an initial dip. To determine
282 this paleoslope, which would explain the low VGP latitudes (see Fig. 8), the
283 magnetic vector v_{GAD} , which would be derived from a GAD, was rotated to
284 the measured vector v_{measured} . The paleodip and paleodip direction describing
285 this rotation were found numerically.

286 For a determination of the measured vector v_{measured} the in situ mean direc-
287 tions were determined for each group of samples, which represent a polarity
288 chron, to randomize the effects of paleosecular variation (see Fig. 8). VGPs
289 from group one do not cluster very well, presumably an effect of the ending
290 of a preceeding reversal. Group two only contains three sites, which is not
291 enough to average out paleosecular variation. The groups three, four and five
292 give good mean directions. However, sites 59-61 were not included into the
293 calculation of the mean direction of group five, because of their excursionsal
294 character. The v_{GAD} for the Neskaupstadur latitude consists of the expected
295 inclination of $I = 77.0$ and declination of $D = 0$. This GAD vector was rotated

296 about all possible paleodips ($0 - \frac{\pi}{2}$) and paleodip directions ($0 - 2\pi$). Thus,
297 the expected $v_{\text{rotated GAD}}$ was determined. The norm of the vector subtraction
298 $|v_{\text{measured}} - v_{\text{rotated GAD}}|$ was calculated and the minimum of the resulting ar-
299 ray (minimum deviation of the two vectors) gives the best-fitting paleodip and
300 paleodip direction (see Tab. 3 and Fig. 8).

301 The determined paleodip directions vary from 4° to 36° and are assumed to
302 represent the flow direction of the flood basalts. By tracking back the direc-
303 tion where the lava flows came from ($184\text{-}216^\circ$) Reydarfjordur central volcano,
304 which is about 15 km away from Neskaupsturdur, might be interpreted as pos-
305 sible extrusion source (see also Fig. 1).

306 However, the calculated paleodips of 19° to 41° are far too high for the slope
307 of central shield volcanoes, which usually have a slope up to 10° (Schmincke,
308 2000). Thus, it has to be assumed, that the observed low VGP latitudes are
309 not solely an effect of the paleoslopes and effects like a regional anomaly or
310 a global field effect have to be taken into account. Remarkably, lower VGP
311 latitudes than expected were not only found in Icelandic lava flows, but as well
312 in the sedimentary datasets of Abdul Aziz et al. (2000) from Calatayud Basin
313 in NE Spain (41.17°N , 1.28°E) and of Hüsing et al. (2007) from northern Italy
314 (43.59°N , 13.56°E), which are of the same age. Despite the remanences of
315 these sediments could be affected by inclination shallowing, all the data from
316 different sites together suggest that the low VGP latitudes are most likely
317 a global field effect. Nevertheless, for a more conclusive statement further
318 datasets, particularly from the southern hemisphere, should be taken into
319 account.

320 **Paleointensity variation between reversals.** For the two lowermost stable
321 polarity intervals too few site were eligible for paleointensity determinations

322 and thus no record of the intensity behavior could be obtained. During the
323 polarity chron C5Ar.1r, the paleointensity builds up from site 18 with $8.5 \mu\text{T}$
324 to site 28 with $39.6 \mu\text{T}$. Above site 35 a large scatter in intensity is observed.
325 Instead of a slow increasing field intensity, the sites 39 ($15.5 \mu\text{T}$) as well as 43
326 ($14.3 \mu\text{T}$) represent low values for a normal polarity interval at high latitudes.
327 The low intensity of site 43 can be interpreted as being related to the onset
328 of the next reversal. During the last reversed polarity chron of this section
329 (C5An.1r) the intensity reaches high values at site 55 ($41.4 \mu\text{T}$). Finally, a low
330 paleointensity value (site 61) during C5An.1r is from a post-excursion site.
331 Overall, the field is characterized by lower paleointensity values compared to
332 the present day field. The VDM, calculated from the paleointensities of the
333 inter-reversal sites, is $3.2 \pm 1.5 \cdot 10^{22} \text{Am}^2$. This is about half of the present
334 dipole moment ($8 \cdot 10^{22} \text{Am}^2$) and even lower the previously published values
335 for the Miocene ($5.9 \pm 0.8 \cdot 10^{22} \text{Am}^2$ (Leonhardt et al., 2000) and $6 \cdot 10^{22} \text{Am}^2$
336 (Juárez et al., 1998)). However, a VDM about $3.2 \cdot 10^{22} \text{Am}^2$ is close to the
337 low-field level of $4 - 5 \cdot 10^{22} \text{Am}^2$ suggested by Shcherbakov et al. (2002) and
338 Heller et al. (2003).

339 *4.2 Transitional fields*

340 **Reversal paths.** Although polarity transitions are geologically spoken so
341 quick that it is difficult to find volcanic rocks that preserve a complete and
342 accurate record, many transitional directions were found in the Nipukollur
343 section. This is surprising looking at the relatively low extrusion rate of ap-
344 proximately one flow per 10 kyr. Fig. 9 shows the VGPs of the four transitions
345 recorded in the sequence. VGPs of contemporary Spanish and Italian data

346 sets (Abdul Aziz et al., 2000; Hüsing et al., 2007) were compared to the re-
347 sults of this study. The oldest reversals C5Ar.2r-C5Ar.1n (see Fig. 9a) is a
348 R-N transition. Prior to the reversed field direction some transitional poles
349 are found east of Patagonia. A first transitional VGP from site 06 is found in
350 Indochina. Sites 07 and 08 show transitional VGP offshore of South Ameri-
351 cas west coast, before reaching the stable field direction in Scandinavia and
352 Siberia. Comparisons to Watkins and Walker (1977) dataset of profile A indi-
353 cate that site 06 is significantly older the sites 07 and 08. Therefore its field
354 direction is assumed to be related to the C5Ar.2n normal chron and not the
355 reversal C5Ar.2r-C5Ar.1n. No transitional directions are found in the Spanish
356 data set (Fig. 9a). The N-R reversal B from C5Ar.1n to C5Ar.1r only contains
357 one clearly transitional data point (site 15) in the middle of the Pacific close
358 to Hawaii (Fig. 9b). Similar Pacific longitudes are observed in the European
359 data which are, however, only weakly defined. A similar post-reversal swing
360 in (Fig. 9b) is found in all three data sets. The R-N reversal C begins with a
361 swing from Antarctica to Australia and back again (site 29). Such directional
362 changes, sometimes referred to as precursors, occasionally accompany reversals
363 (Valet, 2003). After this onset-excursion the VGP path spans straight across
364 the Eastern Pacific and clusters (two lava flows) somewhat south of Hawaii.
365 Such clusters could describe the stop-and-go behavior of reversals (Hoffman,
366 1992) or just be an effect of rapid extrusion of lavas. With East-West swings
367 across Alaska the VGP moves to stable directions in Northern Canada and
368 the Arctic. Similar directions as in the initial excursion and the post-reversal
369 North American VGP cluster are observed in the Italian dataset, suggesting a
370 dipolar dominance during these phases. The last C5An.2n to C5An.1r reversal
371 D (see Fig. 9d) begins in the Arctic Ocean. Then the VGPs cluster near the
372 Ninety-East-Ridge (site 47-49) and move on to Antarctica. Ten lava flows later

373 a post-reversal excursion starts from Antarctica first in the direction of Cape
374 Hope (site 58) but swings on to a near-equatorial VGP near French Polynesia
375 (site 59) and moves on to south of Malaysia (site 60) and near Ninety-East-
376 Ridge (site 61) before coming back to Antarctica. This post-reversal excursion
377 seems to be similar to the termination loops found by Prévot et al. (1985),
378 which show a trend to be anticlockwise in the southern hemisphere (Jacobs,
379 1984). With a last swing to the Amundsen Sea north of Marie Byrd Land (site
380 63 and 64) the sampled section ends. In almost all cases transitional directions
381 can only be found in the final hemisphere, which can be interpreted as a gen-
382 eral trend for the reversals to start pretty fast. This is in good agreement with
383 the observation, that the termination paths are characterized by bigger loops
384 and more intermediate directions than the onset path (Herrero-Bervera, 1986;
385 Jacobs, 1984). A tendency for the Icelandic VGPs to be found in the Pacific
386 (Kristjansson and Jonsson, 2007) can be affirmed with this study (Fig 9).

387 **Intensity variations across a transition.** Unfortunately, below site 18 only
388 few sites were suitable for paleointensity measurements. A general trend of the
389 intensities to decrease during the transitional states (Fig. 5) was found. Dur-
390 ing the reversals A and C the intensity even drops to values below $10 \mu\text{T}$.
391 These observations are in agreement with the common observation that tran-
392 sitions are accompanied by a substantial decrease in the mean intensity of
393 the dipole field (see (Merrill and McFadden, 1999) and references therein).
394 Remarkably the intensity also drops to below-transitional values during the
395 C5An.1n chron. Pre- and post-reversal loops unfortunately yielded no paleoin-
396 tensity data, except for site 61, a post-excursion lava, which is characterized
397 by a low intensity of $6.8 \mu\text{T}$. Despite the high ratio of transitional lavas to
398 non-transitional lavas, none of the four transitions provides a sufficient amount

399 of data to give a detailed picture of the field's intensity behavior during a re-
400 versal. Most likely the frequency of the extrusion of lavas (approximately one
401 lava per 10 kyr) was not high enough to provide a complete record of the
402 field in transition. Furthermore, it is noteworthy that normal polarity results
403 are characterized on average by lower intensity values than reversed polarity
404 lavas.

405 5 Conclusions

406 The Watkins and Walker (1977) profile B in the flood basalt pile near Neskaup-
407 stadur, Eastern Iceland, was resampled and extended about 250 m farther
408 down. The paleomagnetic record of this flood basalt section contains four geo-
409 magnetic field reversals. By correlating the directional data first to the data
410 from Watkins and Walker (1977) and then to the astronomically tuned global
411 timescale (Lourens et al., 2004) the section was identified to range from the
412 reversed C5An.1r chron to the reversed C5Ar.2r and thus cover about 700 kyr
413 of extrusions, approximately between 12.2 and 12.8 Myrs ago. Altogether 18
414 transitional lavas were identified, characterized by a VGP deviation from the
415 geographic poles of more than 41.3° . The paleosecular variation is slightly
416 enhanced in this section. The VGPs during the polarity chrons show a gen-
417 erally lower latitude than expected from a GAD field. Possible reasons for
418 this deviation are related to a local anomaly beneath Iceland, a global field
419 phenomenon and/or non-horizontal flow emplacement. Flood basalts normally
420 flow over very large distances with negligible slope and thus, a bedding cor-
421 rection to the horizontal plane was carried out at first like it is done in most
422 earlier studies. Using a numerical method the paleodip and paleodip direction,

423 which could be responsible for the rotation of the VGPs expected from a GAD
424 to the measured VGPs, were determined. The calculated flow direction points
425 consistently towards a possible volcanic source, the Reydarfjordur central vol-
426 cano. The calculated average paleodip (24.7°), however, seems to be too high
427 for the slope of a central volcano, which usually have a slope of maximum
428 10° . Thus, non-horizontal flow emplacement cannot be the only reason for the
429 observed VGP deviation. Other studies on Mid Miocene sediments of Italy
430 and Spain (Hüsing et al., 2007; Abdul Aziz et al., 2000) also revealed large
431 deviations from the GAD. Thus, the too low VGP latitudes from Iceland are
432 most likely not a local, but a global field effect. This conclusion is also in ac-
433 cordance with the low mean paleointensity of $23.3 \mu\text{T}$ which represents about
434 half of the present field intensity. The saw-tooth pattern (Valet and Mey-
435 nadier, 1993), a fast rebuilding field after the termination of a reversal and a
436 slow decay of the intensity during the polarity interval, was not found during
437 the polarity intervals in this study. Contradicting the saw-tooth hypothesis,
438 the paleointensities would even suggest an inverse feature: an increase of pale-
439 ointensity for one investigated polarity interval(C5Ar.1r). The reversal paths
440 of the VGPs run across the Pacific or Eastern Asia. Generally all paths are
441 in the far-sided hemisphere outside of the proposed longitudinal bands. Other
442 studies on Mid Miocene sediments (Hüsing et al., 2007; Abdul Aziz et al.,
443 2000) also revealed far-sided reversal paths across the Pacific and E-Asia. Due
444 to a low resolution the VGPs paths could not be compared in detail. Never-
445 theless, similar precursors and post-reversal loops were found in all studies,
446 indicating a dipole dominance shortly before and after the reversals. Transi-
447 tional lavas are characterized by a very low paleointensity, below $10 \mu\text{T}$ for
448 two reversals. Altogether, the low intensities and low VGP latitudes suggest a
449 larger influence of non-dipolar terms for Mid Miocene geomagnetic field than

450 compared to today.

451 **Acknowledgements**

We thank Christian Verard, Annika Ferk and Stefan Eder for the help during the field trips. Leo Kristjánsson kindly provided the maps and had helpful suggestions for possible drilling sites. Hayfaa Abdul-Aziz and Silja Hüsing kindly gave access to their data from the Mid Miocene. We thank Pierre Camps and an anonymous reviewer for their helpful and constructive comments. The research was supported through grants from the Deutsche Forschungsgesellschaft (Wi1828/3-1 and So72/67-4).

452 **References**

- 453 Abdul Aziz, H., Hilgen, F., Krijgsman, W., Sanz, E., Calvo, J., 2000. Astro-
454 nomical forcing of sedimentary cycles in the middle to late Miocene conti-
455 nental Calatayud Basin (NE Spain). *Earth Planet. Sci. Lett.* 177, 9–22.
- 456 Camps, P., Henry, B., Nicolaysen, K., Plenier, G., 2007. Statistical properties
457 of paleomagnetic directions in Kerguelen lava flows: Implications for the late
458 Oligocene paleomagnetic field. *J. Geophys. Res.* 112.
- 459 Carmichel, I. S., Turner, F., Verhoogen, J., 1960. *Igneous Petrology*. McGraw-
460 Hill Book Company, Ch. Ferric-ferrous equilibrium in liquids, pp. 282–285.
- 461 Clement, B., 1991. Geographical distribution of transitional VGPs: Evidence
462 for nonzonal equatorial symmetry during the Brunhes-Matuyama geomag-
463 netic reversal. *Earth Planet. Sci. Lett.* 29, 48–58.
- 464 Coe, R. S., Grommé, S., Mankinen, E. A., 1978. Geomagnetic paleointensities

- 465 from radiocarbon-dated lava flows on Hawaii and the question of the Pacific
466 nondipol low. *J. Geophys. Res.* 83, 1740–1756.
- 467 Cox, A., 1969. Confidence limits for the precision parameter k . *Geophys. J.*
468 *R. astr. Soc.* 18, 545–549.
- 469 Day, R., Fuller, M. D., Schmidt, V. A., 1977. Hysteresis properties of titanomag-
470 netites: Grain size and composition dependence. *Phys. Earth Planet.*
471 *Inter.* 13, 260–266.
- 472 Dunlop, D., 2002. Theory and application of the Day plot (M_{rs}/M_s versus
473 H_{cr}/H_c) 1. Theoretical curves and tests using titanomagnetite data. *J. Geo-*
474 *phys. Res.* 107, 10.1029/2001JB000486.
- 475 Fisher, R. A., 1953. Dispersion on a sphere. *Proc. R. Soc. London A* 217,
476 295–305.
- 477 Harrison, C., McDougall, I., Watkins, N., 1979. A geomagnetic field reversal
478 time scale back to 13.0 million years before present. *Earth Planet. Sci. Lett.*
479 42, 143–152.
- 480 Heller, R., Merrill, R. T., McFadden, P. L., 2003. The two states of paleo-
481 magnetic field intensities for the past 320 million years. *Phys. Earth Planet.*
482 *Inter.* 135, 211–223.
- 483 Henry, B., Plenier, G., Camps, P., 2003. Post-emplacement tilting of lava flows
484 inferred from magnetic fabric study: the example of Oligocene lavas in the
485 Jeanne dArc Peninsula (Kerguelen Islands). *Journal of Volcanology and*
486 *Geothermal Research* 127, 153–164.
- 487 Herrero-Bervera, E., Walker, G. P. L., Harrison, C. G. A., Garcia, J. G., Krist-
488 jansson, L., 1999. Detailed paleomagnetic study of two volcanic polarity
489 transitions recorded in eastern Iceland. *Phys. Earth Planet. Inter.* 115, 119–
490 135.
- 491 Herrero-Bervera, E. & Theyer, F., 1986. Non-axisymmetric behavior of Oldu-

- 492 vai and Jaramillo polarity transitions recorded in north-central Pacific deep-
493 sea sediments. *Nature* 332, 159–162.
- 494 Hoffman, K. A., 1992. Dipolar reversal states of the geomagnetic field and
495 core-mantle dynamics. *Nature* 359, 789–794.
- 496 Hüsing, S., Hilgen, F., Abdul Aziz, H., Krijgsman, W., 2007. Completing the
497 Neogene geological time scale between 8.5 and 12.5 Ma. *Earth Planet. Sci.*
498 *Lett.* 253, 340–358.
- 499 Jacobs, J. A., 1984. Reversals of the Earth's magnetic field. Adam Hilger Ltd,
500 Techno House, Redcliff Way, Bristol.
- 501 Juárez, M. T., Tauxe, L., Gee, J. S., Pick, T., 1998. The intensity of the Earth's
502 magnetic field over the past 160 million years. *Nature* 394, 878–881.
- 503 Krafft, M., 1984. Fhrer zu den Vulkanen Europas. Band 1: Allgemeines, Island.
504 Ferdinand Enke Verlag, Stuttgart.
- 505 Kristjansson, L., 1995. New palaeomagnetic results from Icelandic Neogene
506 lavas. *Geophys. J. Int.* 121, 435–443.
- 507 Kristjansson, L., Jonsson, G., 2007. Paleomagnetism and magnetic anomalies
508 in Iceland. *Journal of Geodynamics* , doi:10.1016/j.jog.2006.09.014.
- 509 Laj, C., Mazaud, A., Weeks, R., Fuller, M., Herrero-Bevera, E., 1991. Geo-
510 magnetic reversal paths. *Nature* 351, 447.
- 511 Langereis, C., van Hoof, A. A. M., Rochette, P., 1992. Longitudinal confine-
512 ment of geomagnetic reversal paths as a possible sedimentary artefact. *Na-*
513 *ture* 358, 226–230.
- 514 Leonhardt, R., Fabian, K., 2007. Paleomagnetic reconstruction of the global
515 geomagnetic field evolution during the Matuyama/Brunhes transition: It-
516 erative Bayesian inversion and independent verification. *Earth Planet. Sci.*
517 *Lett.* 253, 172–195.
- 518 Leonhardt, R., Heunemann, C., Krása, D., 2004. Analyzing abso-

- 519 lute paleointensity determinations: Acceptance criteria and the
520 software ThellierTool4.0. *Geochem. Geophys. Geosys.* 5, Q12016,
521 doi:10.1029/2004GC000807.
- 522 Leonhardt, R., Hufenbecher, F., Heider, F., Soffel, H., 2000. High absolute
523 paleointensity during a mid Miocene excursion of the Earth's magnetic field.
524 *Earth Planet. Sci. Lett.* 184, 141–154.
- 525 Lourens, L., F.J., H., Laskar, J., Shackleton, N., Wilson, D., 2004. *A Geological
526 Time Scale 2004.* Cambridge University Press.
- 527 McDougall, I., Schmincke, H.-U., 1976. Geochronology of Gran Canaria, Ca-
528 nary Islands: Age of shield building volcanism and other magmatic phases.
529 *Bull. Volcanol.* 40, 57–77.
- 530 McElhinny, M. W., McFadden, P. L., 1997. Palaeosecular variation over the
531 past 5 Myr based on a new generalized database. *Geophys. J. Int.* 131,
532 240–252.
- 533 McFadden, P. L., McElhinny, M. W., 1988. The combined analysis of remagne-
534 tization circles and direct observations in palaeomagnetism. *Earth Planet.
535 Sci. Lett.* 87, 161–172.
- 536 Merrill, R. T., McFadden, P. L., 1999. Geomagnetic polarity transitions. *Rev.
537 Geophys.* 37, 201–226.
- 538 Opdyke, N., 1972. Paleomagnetism of deep sea cores. *Reviews of Geophysics
539 and Space physics* 10, 213–249.
- 540 Prévot, M., Camps, P., 1993. Absence of preferred longitude sectors for poles
541 from volcanic records of geomagnetic reversals. *Nature* 366, 53–57.
- 542 Prévot, M., Mankinen, E. A., Coe, R. S., Grommé, S., 1985. The Steens Moun-
543 tain (Oregon) geomagnetic polarity transition 2. Field intensity variations
544 and discussion of reversal models. *J. Geophys. Res.* 90, 10417–10448.
- 545 Roberts, A. P., Winklhofer, M., 2004. Why are geomagnetic excursions not

- 546 always recorded in sediments? Constraints from post-depositional remanent
547 magnetization lock-in modelling. *Earth Planet. Sci. Lett.* 227, 345–359.
- 548 Schmincke, H., 2000. *Vulkanismus*. Wissenschaftliche Buchgesellschaft.
- 549 Shcherbakov, V. P., Solodovnikov, G. M., Sycheva, N. K., 2002. Variations in
550 the geomagnetic dipole during the past 400 million years (Volcanic rocks).
551 *Izv. Acad. Sci. USSR Phys. Solid Earth, Engl. Trans.* 38, 113–119.
- 552 Tauxe, L., August 1993. Sedimentary records of the relative paleointensity of
553 the geomagnetic field: Theory and practice. *Rev. Geophys.* 31, 319–354.
- 554 Tric, E., Laj, C., Valet, J.-P., Tucholka, P., Paterna, M., Guichard, F., 1991.
555 The Blake geomagnetic event: transition geometry, dynamical characteris-
556 tics and geomagnetic significance. *Earth Planet. Sci. Lett.* 102, 1–13.
- 557 Valet, J.-P., 2003. Time variations in geomagnetic intensity. *Rev. Geophys.*
558 41, doi:10.1029/2001RG000104.
- 559 Valet, J.-P., Brassart, J., Le Meur, I., Soler, V., Quidelleur, X., Tric, E., Gillot,
560 P.-Y., 1996. Absolute paleointensity and magnetomineralogical changes. *J.*
561 *Geophys. Res.* 101 (B11), 25029–25044.
- 562 Valet, J.-P., Meynadier, L., November 1993. Geomagnetic field intensity and
563 reversals during the past four million years. *Nature* 366, 234–238.
- 564 Walker, G., 1964. Geological investigations in eastern Iceland. *Bulletin of Vol-*
565 *canology* 27, 351–361.
- 566 Walker, G., 1974. NATO advanced study institutes series, Series C “Mathe-
567 matical and Physical Series, Vol.11 Geodynamics of Iceland and the North
568 Atlantic Area. Dordrecht, Reidel, Netherlands, Ch. The Structure of East-
569 ern Iceland, pp. 177–188.
- 570 Watkins, N., Walker, G. P. L., 1977. Magnetostratigraphy of eastern Iceland.
571 *Am. J. Sci.* 277, 513–584.

Fig. 1. **Left:** Sampled section as seen from the lighthouse of Neskaupstadur. Original profile B of Watkins and Walker (1977) indicated with the dashed line. The bold line marks the sampled section of this study. **Right:** Overview about previous paleomagnetic projects in Eastern Iceland (modified after Kristjansson (1995)).

Fig. 2. Day plot (Day et al., 1977) with mixture lines and boundary values according to Dunlop (2002). The samples cluster within the PSD range along the SD-MD mixture lines.

Fig. 3. Ore microscopy of samples from different rock magnetic groups: Group 1 contains 5 % of samples, group 2 10 %, group 3 25 % and group 4 60 %. Samples were covered with ferrofluid, except right picture of group 2 and the group 3 picture, which were examined under polarized light.

Fig. 4. Orthogonal projections of **a)** stable directions (Site 28 with reversed polarity, 46 with normal polarity and transitional JD transitional) and **b)** great circle (Site 46B) and **c)** rejected samples (Site 10)

Fig. 5. Paleodirections (declination and inclination) for each sampled site and absolute paleointensities for eligible sites versus altitude. The dashed lines denote the values expected from a GAD. The polarity log was generated using a cut-off colatitude of 41.3° (McElhinny and McFadden, 1997) with black for normal, white for reversed and grey for transitional lava flows. Reversals are numbered from A to D and polarity chrons denoted after global timescale (for correlation see Fig. 7.)

Fig. 6. Arai plots of site 12 and 25 together with orthogonal projections (black circle for declination and white circle for inclination). The dashed lines indicate the linear segment used for the calculation of paleointensity. Triangles denote the alteration check step, gray squares the additivity checks.

Fig. 7. Correlation of VGPs to the results of Watkins and Walker (1977) and to global timescales like the ATNTS of Lourens et al. (2004).

Fig. 8. Trend of VGPs to lower latitudes for the lower section of the profile. The grey line shows the bedding corrected data with the values of the regional tilt, the black line the in situ data. The mean VGP latitudes are calculated for each group of stable field directions and given in Tab. 3. The mean inclination is shown with a black star. Results of the MATLAB™ calculations of the paleoslope are shown for each group. See text for more information.

Fig. 9. VGP paths projected on the globe for transitions in the Neskaupstadur/Nipukollur section. **a)** is the oldest R-N transition, **d)** the youngest N-R transition. The black star denotes the Icelandic site. The dashed grey lines is based on the Spanish data set, the pointed dark grey on the Italian data set.

Table 1: Directional results

Site	Altitude [m]	n/N	D _g [°]	I _g [°]	D _s [°]	I _s [°]	k	α ₉₅ [°]	F [μT]	VGP long. [°]	VGP lat. [°]	Pol.	
64	761	6/6	268.2	-76.6	270.0	-80.6	490	3.0			204.6	-59.5	R
63	740	5/6	296.8	-72.9	305.5	-76.1	173	5.8			197.0	-44.8	T
62	735	5/6	198.5	-79.9	175.4	-80.8	49	11.1			154.8	-82.9	R
61	731	5/6	84.4	-50.7	84.4	-46.7	309	4.4	6.8		93.7	-22.9	T
60	727	4/5	66.2	-44.5	67.3	-40.7	326	5.1			106.3	-12.1	T
59	718	5/6	287.7	-49.5	289.8	-53.1	485	3.5			224.4	-22.6	T
58	713	6/7	159.6	-56.0	154.1	-54.8	90	7.1			26.5	-56.4	R
57	703	6/6	183.3	-74.2	169.1	-74.4	161	5.3			40.1	-83.4	R
56	684	4/6	174.6	-76.7	158.1	-76.2	230	6.1			78.4	-80.5	R
55	681	6/6	159.5	-83.1	133.5	-81.2	1919	2.5	41.4		121.6	-72.3	R
54	675	7/7	275.7	-80.9	284.5	-84.8	253	3.8			187.2	-60.9	R
53	669	7/7	265.4	-80.6	266.4	-84.6	487	2.7			191.1	-63.7	R
52	660	6/6	264.9	-76.8	265.3	-80.8	182	5.0	37.8		205.5	-60.9	R
51	652	6/6	225.9	-78.9	208.8	-81.7	328	3.7	25.1		203.1	-77.0	R
50	629	5/5	162.8	-67.2	153.9	-66.1	61	9.9			38.6	-68.3	R
49	619	5/6	111.4	-54.4	109.1	-50.8	72	9.1			74.0	-36.3	T
48	616	5/5	81.6	-47.3	81.8	-43.3	75	8.9			94.6	-19.4	T
47	612	4/4	75.5	-37.8	75.9	-33.8	150	10.3			96.8	-11.0	T
46B*	609	0/4											
46	606	6/6	356.7	80.0	334.8	79.4	235	4.4	23.3		291.6	79.5	N
45 (EB21)	598	6/6	355.8	75.2	337.4	74.5	47	9.9			244.5	79.0	N
44 (EB20)	595	6/6	44.6	69.0	34.5	72.6	308	3.8			84.1	72.3	N
43	592	6/6	47.0	75.0	32.0	78.6	55	9.1	14.3		49.2	77.1	N
42	590	6/6	25.9	79.2	358.7	80.8	176	5.1	32.5		343.0	83.1	N
41	586	5/5	348.4	75.9	329.9	74.6	237	5.0			253.8	76.0	N
40	585	6/6	313.8	77.4	300.5	73.7	278	4.0	26.0		273.0	63.0	N
39	583	6/7	351.6	60.9	342.8	60.3	496	3.0	15.5		197.0	64.2	N
38	571	5/5	340.6	73.1	326.0	71.3	76	9.1			243.1	71.2	N
37	566	6/6	309.1	75.3	298.4	71.4	226	4.5	25.5		268.7	59.8	N
36	562	6/6	347.5	52.7	341.1	51.9	101	6.7			195.1	55.4	N
35 (EB14)	551	4/5	349.8	50.0	343.9	49.4	755	3.3	10.4		190.2	53.7	N
34	540	0/6											
33	538	6/6	318.5	18.1	317.3	15.2	40	10.8			214.4	25.3	T
32 (EB10)	488	6/6	316.6	30.4	314.4	27.3	278	4.0	5.8		220.0	30.8	T
31	472	5/5	186.0	-62.8	176.2	-63.4	135	6.6	9.0		354.1	-69.7	R
30*	469	0/4											
29 (EB7)	463	5/5	44.1	-61.0	49.2	-57.0	133	7.1			126.8	-19.6	T
28 (EB6C)	460	5/6	204.3	-57.3	197.0	-59.5	354	4.1	39.6		316.6	-63.3	R
27	455	6/6	196.8	-59.4	188.5	-61.0	152	5.9			330.4	-66.4	R
25	443	6/7	203.3	-61.7	192.5	-64.1	154	5.4	25.0		320.8	-69.5	R
24	424	6/6	238.5	-76.2	221.6	-81.2	137	5.9	23.4		210.7	-73.7	R
23B	420	5/6	247.5	-65.4	242.6	-71.1	127	6.8			243.9	-59.1	R
23	418	5/5	186.3	-83.5	138.2	-82.2	123	7.4			128.5	-73.3	R
22	410	5/5	157.8	-51.1	151.0	-49.1	205	5.4			27.7	-50.5	R
21	406	4/6	156.2	-48.0	150.2	-45.9	179	6.9	14.8		27.4	-47.7	T
20	401	6/6	202.1	-76.6	175.9	-78.2	229	4.4			130.9	-87.3	R
19 (EB1)	398	6/6	177.2	-65.0	164.4	-64.7	95	6.9			18.4	-69.6	R
18	388	5/6	191.8	-64.4	179.2	-65.6	65	9.6	8.5		348.1	-72.6	R
17	383	6/6	200.9	-62.0	189.9	-64.2	60	8.7			325.8	-70.1	R
16	378	5/5	215.9	-75.6	193.1	-78.7	66	9.5			219.9	-84.0	R
15	373	6/6	338.2	8.5	337.4	6.8	74	7.8			191.7	26.2	T
14	372	6/6	49.7	70.6	37.0	75.2	206	4.7			69.7	73.6	N
12	310	6/6	62.6	67.6	55.5	73.1	42	10.4	7.3		64.2	64.0	N
11	307	6/6	80.8	77.6	77.8	83.6	97	6.8			16.5	64.8	N
10	272	0/7											
09	269	0/6											
08	266	3/3	267.7	-4.7	267.8	-11.7	194	8.9			255.8	-6.3	T
07	265	5/5	246.7	-19.1	245.8	-25.8	100	8.8			272.9	-22.4	T
06	245	6/6	60.1	18.3	59.0	24.7	55	9.3	6.8		99.7	24.5	T
05	240	6/7	276.5	-73.8	285.5	-80.5	123	6.1	15.7		199.1	-55.6	R
04	235	0/3											
03	233	7/7	281.6	-76.5	298.6	-82.9	97	6.2	16.1		188.8	-56.3	R
02	229	7/7	262.0	-70.0	261.0	-77.0	187	4.4	48.7		218.5	-58.4	R
01	227	8/8	254.0	-67.7	249.7	-74.5	99	5.6			231.1	-59.8	R
00	222	6/6	237.3	-68.5	226.1	-74.4	59	8.8			246.6	-69.1	R
JA	217	6/6	229.9	-51.7	224.0	-57.3	267	4.1	20.4		281.5	-52.8	R
JB	214	5/5	215.9	-41.8	210.7	-46.2	65	9.6	22.8		304.1	-47.7	T
JC	209	6/6	207.1	-32.9	202.9	-36.5	1385	1.8	14.3		316.6	-42.7	T
JD	199	5/6	211.3	-26.8	208.2	-30.9	167	5.9	22.0		311.3	-37.9	T
Dykes:													
13	312	5/8	19.0	44.8	13.3	47.1	52	10.7			147.0	52.2	N

Table 1: Directional results

Site	Altitude [m]	n/N	D_g [°]	I_g [°]	D_s [°]	I_s [°]	k	α_{95} [°]	F [μ T]	VGP long. [°]	VGP lat. [°]	Pol.
DY	205	5/5			1.3	73.1	148	6.3		160.3	83.5	N

Directional results for all sampled sites. Altitudes (GPS-altitudes in normal fonts, italics for interpolated altitudes), n/N is the number of samples used for the calculation of the mean directions versus the number of samples treated, D_g and I_g denote declination and inclination in geographic coordinates, D_s and I_s the declination and inclination in stratigraphic coordinates, k and α_{95} indicate the concentration parameter and the confidence cone, F yields the weighted mean intensity of all suitable specimens of a site (see Table 2), VGP longitude and latitude give the coordinates of the virtual geomagnetic pole. The polarity of each flow are given with N for normal polarity, R for reversed and T for transitional (if the VGP latitude is below 48.7° (McElhinny and McFadden, 1997)). A * following the sample name denotes transitional lava flows, which could only be evaluated with great circle analysis. Based on flow descriptions, similar altitude, and their position relative to pronounced red beds, some lava flows could be unambiguously correlated to profile B of Watkins and Walker (1977). In this case the site name used by Watkins and Walker (1977) is given in parenthesis after our site name. Above and below these flows a direct flow-to-flow correlation between Watkins and our work is not possible, because of slightly different sampling routes. Comparison, however, is possible based on altitude measurements.

572

Table 2: Paleointensity results of Neskaupstadur section

Site	Alt.	n/N	Sample	T_{min}	T_{max}	N	f	g	q	w	F_i	σF_i	F	σF
64	761	0/2												
61	731	3/3	61-1*	400	580	7	0.79	0.72	24.8	11.1	7.2	0.2	6.8	0.3
			61-4*	400	580	7	0.79	0.71	21.6	9.6	6.4	0.2		
			61-5	430	610	7	0.85	0.75	11.0	4.9	6.9	0.4		
55	681	5/5	55-1	280	580	10	0.89	0.77	20.2	7.1	29.8	1.0	41.4	4.1
			55-2	100	520	15	0.48	0.84	6.0	1.7	47.2	3.1		
			55-3	310	520	7	0.37	0.80	4.6	2.0	37.5	2.4		
			55-4	100	490	13	0.44	0.88	39.1	11.8	45.4	0.5		
			55-5	200	490	8	0.46	0.82	10.6	4.3	47.1	1.7		
52	660	2/4	52-2*	200	460	7	0.33	0.80	2.6	1.2	29.7	3.0	37.8	6.3
			52-4	490	610	5	0.83	0.65	27.6	16.0	38.6	0.8		
51	652	3/3	51-2	370	610	9	0.90	0.76	18.3	6.9	21.4	0.8	25.1	1.9
			51-3*	400	610	8	0.86	0.82	20.2	8.3	27.6	1.0		
			51-6*	370	550	7	0.82	0.78	14.8	6.6	26.2	1.1		
49	619	0/2												
46	606	3/3	46-3*	490	610	5	0.66	0.58	13.3	7.7	19.4	0.6	23.3	1.5
			46-5	390	580	7	0.88	0.77	24.8	11.1	22.5	0.6		
			46-4	20	580	13	0.96	0.82	37.7	11.4	25.2	0.5		
43	592	3/3	43-2*	200	610	12	0.96	0.81	25.9	8.2	14.8	0.4	14.3	0.8
			43-3*	490	610	5	0.58	0.56	20.4	11.8	13.2	0.2		
			43-6	20	490	10	0.32	0.76	2.6	0.9	17.5	1.6		
42	590	3/3	42-3	20	520	16	0.67	0.90	32.0	8.5	31.7	0.6	32.5	2.6
			42-4*	190	520	11	0.77	0.88	5.1	1.7	42.8	5.7		
			42-6*	220	430	8	0.42	0.84	10.4	4.3	29.7	1.0		
41	586	0/3												
40	585	2/2	40-3	20	490	10	0.41	0.77	2.3	0.8	21.9	3.0	26.0	7.0
			40-6	100	460	8	0.30	0.83	2.4	1.0	29.9	3.1		
39	583	2/2	39-4	100	490	9	0.33	0.81	3.0	1.1	14.8	1.3	15.5	2.1
			39-6*	100	490	9	0.32	0.83	3.1	1.2	16.2	1.4		
38	571	0/3												
37	566	2/3	37-1	20	350	6	0.38	0.77	3.0	1.5	26.4	2.6	25.5	2.8
			37-6*	20	460	9	0.75	0.86	9.2	3.5	25.2	1.8		
36	562	0/3												
35	551	3/3	35-1	350	610	9	0.98	0.80	12.8	4.8	8.4	0.5	10.4	1.1
			35-3*	200	610	12	0.97	0.80	38.5	12.2	11.4	0.2		
			35-4*	250	520	8	0.56	0.76	3.4	1.4	7.1	0.9		
32	488	4/4	32-1	300	610	10	1.00	0.82	6.7	2.4	4.9	0.6	5.8	0.8
			32-3	220	580	12	0.85	0.77	11.4	3.6	6.6	0.4		
			32-4*	220	580	12	0.95	0.81	3.7	1.2	8.3	1.7		
			32-6	370	610	9	0.90	0.84	8.0	3.0	4.3	0.4		
31	472	3/4	31-2*	370	580	7	0.77	0.76	8.9	4.0	12.9	0.9	9.0	1.9
			31-4	370	580	7	0.75	0.71	14.4	6.4	8.3	0.3		
			31-5	370	520	5	0.41	0.61	7.0	4.0	5.7	0.2		
28	460	5/6	28-1	20	610	14	0.96	0.84	31.5	9.1	34.7	0.9	39.6	3.3
			28-2	200	430	6	0.31	0.77	6.1	3.0	42.6	1.7		
			28-3*	200	610	12	0.95	0.76	81.1	25.6	44.5	0.4		
			28-5	300	610	10	0.94	0.81	25.0	8.8	30.4	0.9		
			28-6*	350	610	9	0.99	0.78	7.8	2.9	36.1	3.6		
27	455	0/3												
25	443	4/4	25-3	350	610	9	0.93	0.81	20.9	7.9	25.4	0.9	25.0	0.2
			25-2	350	610	9	0.92	0.76	9.2	3.5	25.1	1.9		
			25-7*	430	610	7	0.78	0.70	10.9	4.9	24.8	1.3		
			25-5*	200	610	12	0.94	0.82	18.5	5.8	24.5	1.0		
24	424	3/4	24-1*	350	610	9	0.92	0.75	17.7	6.7	24.9	1.0	23.4	0.8
			24-4	20	350	6	0.62	0.76	3.6	1.8	22.9	3.0		
			24-6*	250	610	11	0.93	0.76	25.5	8.5	22.4	0.6		
23	418	0/3												
21	406	2/3	21-1	490	610	5	0.74	0.67	23.6	13.6	17.2	0.4	14.8	2.4
			21-2	390	610	8	0.89	0.72	31.7	13.0	13.1	0.3		
20	401	0/2												
18	388	3/4	18-1	310	520	7	0.36	0.76	5.8	2.6	10.7	0.5	8.5	2.0
			18-3	370	580	8	0.86	0.78	9.4	3.9	5.7	0.4		
			18-5*	130	280	6	0.33	0.75	4.0	2.0	12.1	0.7		
12	310	4/4	12-2	20	580	17	0.90	0.78	14.6	3.8	7.7	0.4	7.3	0.3
			12-3	220	550	11	0.84	0.76	8.1	2.7	6.8	0.5		
			12-4	340	520	6	0.48	0.65	4.3	2.1	8.1	0.6		
			12-6	220	550	11	0.84	0.74	18.7	6.2	7.1	0.2		
07	265	0/1												
06	245	3/4	06-2	490	610	5	0.82	0.69	29.8	17.2	8.0	0.2	6.8	0.7
			06-3*	300	610	10	0.92	0.61	28.3	10.0	6.7	0.1		
			06-4*	460	610	6	0.85	0.65	21.7	10.9	5.4	0.1		
05	240	2/2	05-4	20	490	10	0.35	0.74	2.5	0.9	18.6	1.9	15.7	4.4
			05-2	200	520	9	0.55	0.74	3.1	1.2	13.5	1.8		
04	235	0/3												

Table 2: Paleointensity results of Neskaupstadur section

Site	Alt.	n/N	Sample	T_{min}	T_{max}	N	f	g	q	w	F_i	σF_i	F	σF
03	233	2/4	03-1	20	550	12	0.58	0.86	10.9	3.4	13.6	0.6	16.1	2.7
			03-5*	430	610	7	0.87	0.69	16.4	7.3	17.8	0.7		
02	229	3/4	02-4*	100	580	16	0.94	0.78	25.3	6.8	53.2	1.5	48.7	2.8
			02-5*	310	550	8	0.91	0.73	12.6	5.1	46.9	2.5		
			02-7	370	580	7	0.87	0.78	23.0	10.3	44.7	1.3		
ja	217	4/4	ja-1	460	610	6	0.91	0.60	14.2	7.1	20.8	0.8	20.4	0.6
			ja-2*	490	610	5	0.78	0.56	48.3	27.9	20.4	0.2		
			ja-3	460	610	6	0.91	0.62	12.6	6.3	22.2	1.0		
			ja-4	490	610	5	0.86	0.57	14.4	8.3	18.2	0.6		
jb	214	4/4	jb-1	200	610	12	1.00	0.84	7.0	2.2	24.8	3.0	22.8	1.9
			jb-2	430	610	7	0.95	0.68	29.5	13.2	23.2	0.5		
			jb-3	490	610	5	0.88	0.57	14.8	8.6	18.0	0.6		
			jb-4	250	430	5	0.33	0.69	7.5	4.3	28.5	0.9		
jc	209	4/4	jc-1*	20	610	14	0.99	0.77	26.7	7.7	15.0	0.4	14.3	1.0
			jc-3	20	550	12	0.82	0.64	7.2	2.3	14.6	1.1		
			jc-4	460	610	6	0.74	0.68	8.8	4.4	10.7	0.6		
			jc-5*	250	490	7	0.40	0.80	4.7	2.1	16.6	1.2		
jd	199	4/4	jd-3*	490	610	5	0.70	0.67	20.8	12.0	19.1	0.4	22.0	1.4
			jd-4	250	550	9	0.84	0.81	32.5	12.3	22.4	0.5		
			jd-5	20	350	6	0.37	0.78	3.7	1.8	21.9	1.7		
			jd-6	490	610	5	0.88	0.67	10.4	6.0	26.4	1.5		

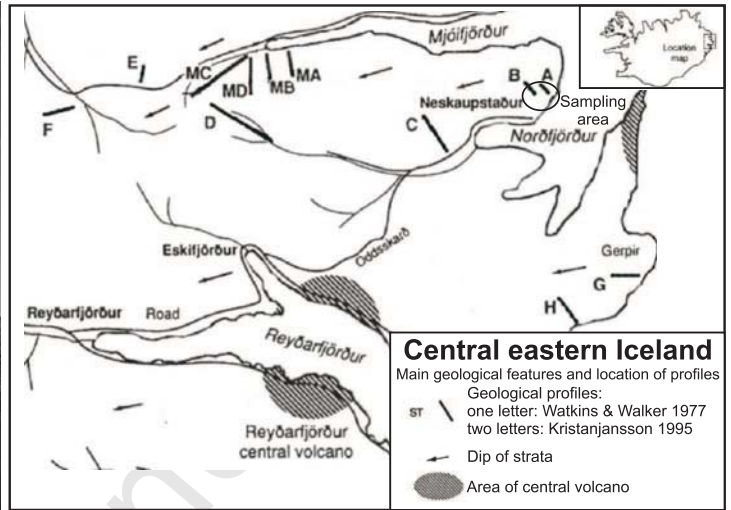
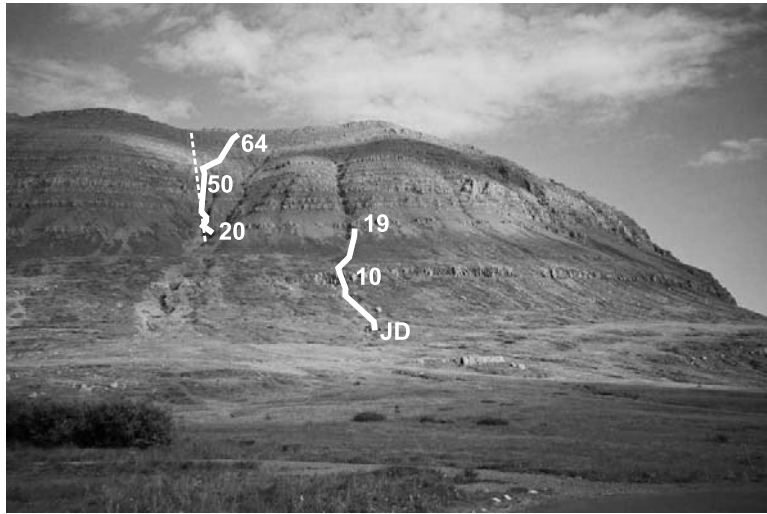
Site denotes the flow number and Alt their altitude in the profile. The success rate n/N is the number of successful measured samples per site versus the number of treated specimen. The sample name is extended by a superscripted star in case of check corrected analysis. T_{min} and T_{max} give the temperature interval used for the paleointensity calculations. N gives the number of successive data points in the used interval, f gives the used fraction of the NRM, g the gap factor and q the quality factor. The weighting factor is denoted w. F_i and σF_i give the paleointensity and its standard deviation for each single sample, F gives the weighted mean from the individual paleointensity measurements weighted with the quality factor q and the weighted standard deviation sigma F. If a site only contains two evaluable samples the minimum-maximum deviation was calculated instead of a weighted standard deviation.

Table 3

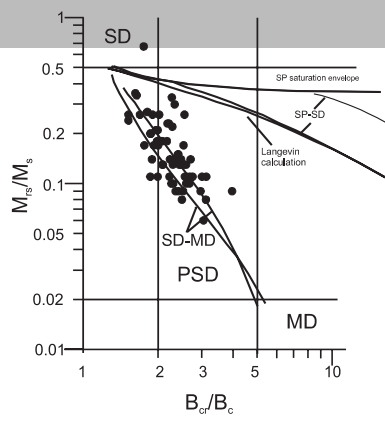
Paleodip and its direction. N denotes the number of flows used for the calculation.

Group (Sites)	N	Mean D/I	α_{95}	k	paleodip	paleodip direction
1 (jd-05)	9	229.6/-59.1	15.1	12.6	41	36
2 (11-14)	3	62.2/72.3	10.3	144.0	15	<i>107</i>
3 (16-31)	12	202.9/-68.6	6.0	53.0	34	14
4 (34-45)	10	358.1/76.3	6.1	63.2	3	4
5 (50-62)	8	233.8/-81.8	5.5	103.9	19	16
Mean					24.7	16.4

The dip direction of group 2 is printed italic, as only three sites contribute to the group mean direction. Therefore this result is assumed to be unreliable.

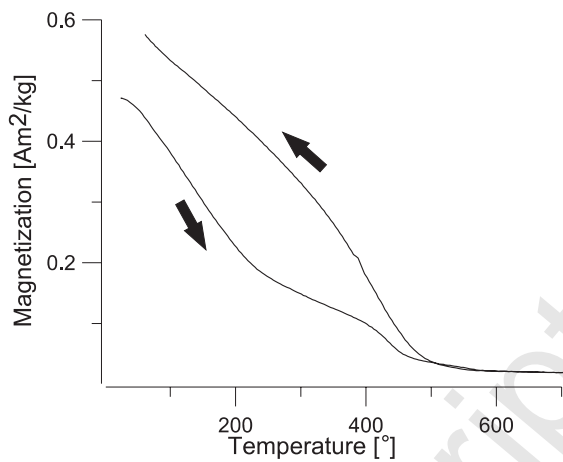
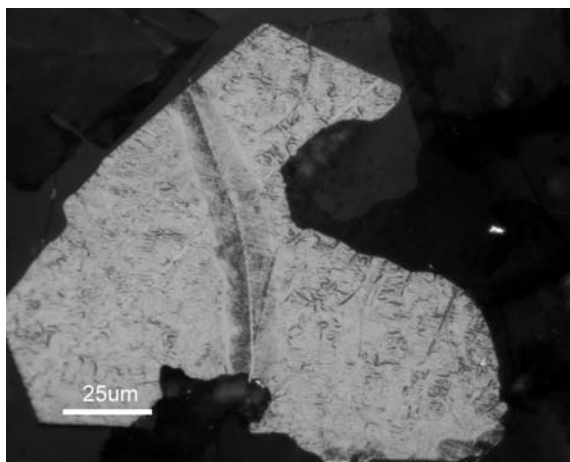


Accepted Manuscript

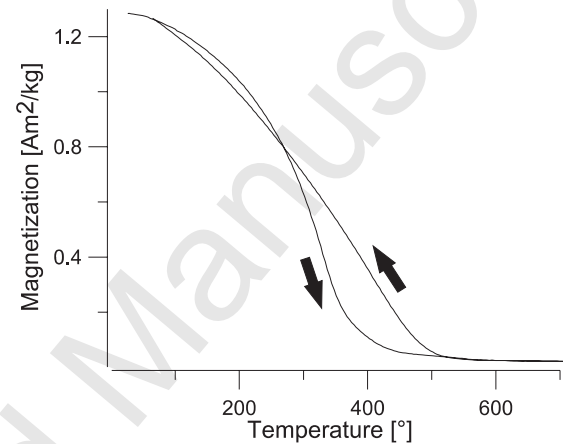
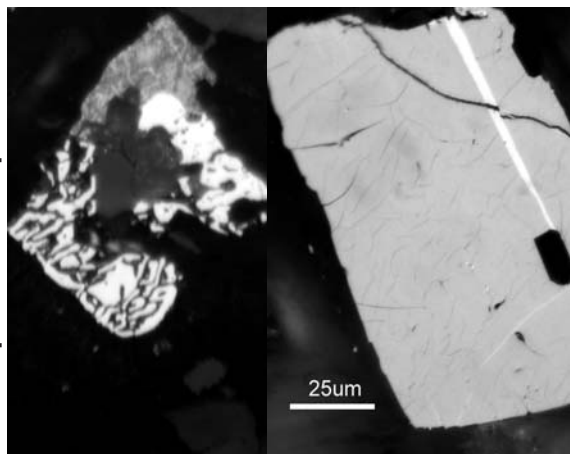


Accepted Manuscript

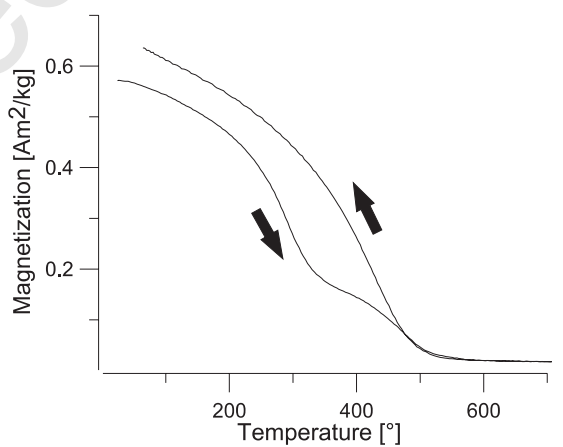
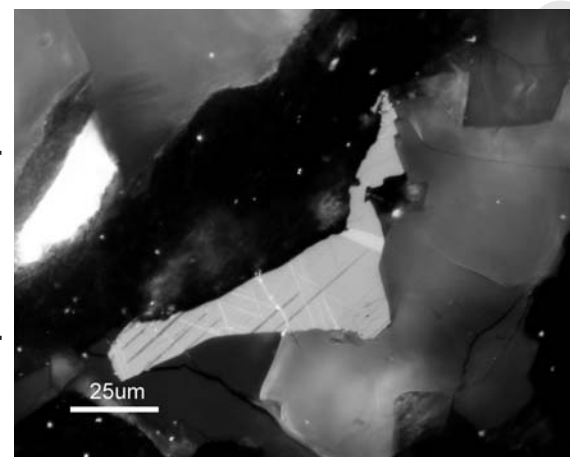
Group 1: Sample 59



Group 2: Sample 47



Group 3: Sample 02



Group 4: Sample 32

